Progress In Electromagnetics Research Letters, Vol. 73, 113–120, 2018

A Compact Dual-Element Uniplanar Antenna for Portable Broadband MIMO Systems

Aliakbar Dastranj*

Abstract—A printed dual-port coplanar waveguide (CPW)-fed antenna is proposed for wideband communication systems. The antenna includes two identical hybrid trapezoidal-elliptical radiating elements that are printed perpendicular to each other. Also, two orthogonal CPW lines are used to feed the antenna. In order to achieve broadband dual-polarized operation with a compact size, the geometrical parameters of the antenna are optimized by using Ansoft HFSS. The antenna was fabricated and tested. Reasonable agreement between the simulation and experimental results is obtained. The fabricated prototype with a small size of $25 \times 53\,\text{mm}^2$ can cover the wide operating frequency band from 2.4 to 18 GHz (reflection coefficient less than -10 dB) for both ports. The measured isolation is better than 25 dB over the entire operating bandwidth. Moreover, the measured results show that the proposed antenna can provide omnidirectional radiation patterns with a good orthogonal polarization operation, reasonable gain, high radiation efficiency, and constant group delay.

1. INTRODUCTION

The fading of ultra-wideband (UWB) signals due to multipath environment is the main drawback of the conventional single-antenna communication systems [1]. Multiple-input multiple-output (MIMO) technology is one of the suitable techniques to reduce multipath phenomenon in complex environment and increase capacity, spectral efficiency, and reliability of the communication channel [2–6]. The UWB-MIMO systems require multiple wideband antennas with good isolation performance between antenna ports. In an environment of limited space, MIMO system can be accomplished by utilizing the independence of the propagation paths of the two different polarizations [7]. An analytical framework for accessing MIMO system was presented in [8]. In [9], by exploiting multiple polarizations with a tri-monopole antenna, the channel capacity of MIMO system was simulated. It was shown that the increase in channel capacity is due mainly to polarization diversity, not pattern diversity.

Over the past few years several types of wideband MIMO antennas have been proposed [10–20]. A compact and low-correlation MIMO antenna system covering 1710–2690 MHz band with 12 dB isolation for wireless communication standards was proposed in [10]. The design of a compact four E-shaped patch element MIMO antenna at 5.8 GHz by using the invasive weed optimization algorithm was proposed in [11]. In [12], by using induced emf method and transmission line model, a two-probe excited circular ring antenna for a long and narrow environment. The design process was to choose a suitable radius of the ring for a single probe antenna. Then, the suitable probe length and ring length were determined for the two-probe antenna and isolation between the two probes was enhanced by insertion of an inductor coil between the probes. The antenna achieved isolation in excess of 20 dB and VSWR less than 2 : 1 at the frequency of 5.2 GHz and a bidirectional radiation pattern with 4 dBi gain. Various isolation improvement techniques for MIMO WLAN card bus applications including planar ground strips, band-notched ground slits, resistive cards between the antenna elements and possible combinations of the

Received 9 January 2018, Accepted 2 February 2018, Scheduled 2 March 2018
* Corresponding author: Aliakbar Dastranj (dastranj@yu.ac.ir).
The author is with the Department of Electrical Engineering, Faculty of Engineering, Yasouj University, Yasouj, Iran.

above were presented in [13]. In [14], a CPW-fed planar Cantor set fractal antenna with spatial diversity performance covering the frequency range from 4.5 to 10.6 GHz was presented. By etching multiple slots in its ground plane a good isolation better than 20 dB was achieved. In [15], a compact UWB dual-port spatial diversity antenna with a size of $27 \times 47\,\mathrm{mm}^2$ can provide the working band of 2.2–11 GHz. The mutual coupling between its ports is below 15 dB across the whole frequency range. In [16], a dual-port CPW-fed printed antenna with a size of $56 \times 56\,\mathrm{mm}^2$ was proposed. It consists of two uniform right angled triangular radiation patches and a triangular slot. It provides port isolation more than 20 dB over the frequency of 3-10.8 GHz. In order to decrease the mutual coupling between the ports a slant metal strip was printed in the middle of the triangular slot. An annular slot antenna with the frequency range of 3-12 GHz was proposed for pattern diversity operation [17]. Its port isolation is above 15 dB. However, it has a relatively large size of $80 \times 80\,\mathrm{mm}^2$ which is not appropriate for use in portable devices. In [18], an UWB monopole antenna with a total size of $34 \times 49\,\mathrm{mm}^2$ and the operational frequency range of 3.1–10.6 GHz was presented for polarization diversity applications. It features good isolation performance above 20 dB across the entire band of interest. To achieve this wideband operation, a heptagonal radiator, a modified CPW feed-line, and an extended ground plane were proposed. A printed single-layer CPW-fed polarization diversity monopole-like slot antenna with a size of $50 \times 50\,\mathrm{mm}^2$ was presented in [19]. To obtain good isolation between the ports, a strip was integrated diagonally in the ground plane. It provides good impedance matching and isolation better than 15 dB across the frequency range from 2.76 to 10.75 GHz whereas showing the rejection performance in the sub band of 4.75–6.12 GHz. The dual-port CPW-fed polarization diversity antenna presented in [20] with good port isolation better than 22 dB and small size of $27 \times 52\,\mathrm{mm}^2$ has the impedance bandwidths of 115% (3.25–12 GHz) and 107% (3.55–11.7 GHz) for port 1 and port 2, respectively.

In this research, a compact and broadband uniplanar dual-port antenna is proposed. The antenna consists of two exactly the same hybrid trapezoidal-elliptical radiating patches that are printed perpendicular to each other. Also, two orthogonal CPW lines are used to feed the patches. The fabricated prototype with a small size of $25 \times 53\,\mathrm{mm}^2$ has the broad working band from 2.4 to 18 GHz (reflection coefficient less than -10 dB) for both ports. The novelty of the proposed design lies in its simple configuration and simplicity to obtain the desired antenna characteristics in both time- and frequency-domain. Notice that compared to the previous work in [21], the designed antenna has a simpler structure and wider operating bandwidth. The measured isolation between the ports is above 25 dB across the entire band of interest. Moreover, the proposed antenna can provide omnidirectional radiation patterns with a good orthogonal polarization operation, reasonable gain, high radiation efficiency, and constant group delay. Compared to the recent designs reported in [16–20], the proposed antenna features broader overall bandwidth, better port isolation, and smaller size, simultaneously. This comparison reveals the advantages of the antenna. Measured results in both time- and frequency-domain show that the antenna is an attractive candidate for use in portable MIMO devices.

2. ANTENNA DESIGN

The geometry and fabricated prototype of the proposed antenna are illustrated in Figure 1. The antenna includes two identical hybrid trapezoidal-elliptical monopoles that are printed perpendicular to each other and orthogonally fed by two $50\,\Omega$ CPW lines. The spacing between the two monopole is $S = 4.3\,\mathrm{mm}$. The orthogonal placement of the feeding structures accomplishes the dual polarization performance of the antenna. The antenna is printed on an FR4 substrate of a relative permittivity $\varepsilon_r = 4.4$ and thickness $h = 1.2\,\mathrm{mm}$ with total area of $25 \times 53\,\mathrm{mm}^2$. In order to achieve compact size and broadband dual-polarized performance, the design parameters of the antenna are optimized by using Ansoft HFSS. The optimal geometrical parameters of the antenna are as follows: $w = 25\,\mathrm{mm}$, $l = 53\,\mathrm{mm}$, $r_1 = 8.7\,\mathrm{mm}$, $r_2 = 6.53\,\mathrm{mm}$, $d = 0.5\,\mathrm{mm}$, $l_p = 13.2\,\mathrm{mm}$, $w_p = 24.5\,\mathrm{mm}$, $w_g = 10\,\mathrm{mm}$, $l_g = 11.4\,\mathrm{mm}$, $w_f = 1.6\,\mathrm{mm}$, and $g = 0.3\,\mathrm{mm}$. Each hybrid patched of the antenna consists of elliptical and trapezoidal sections, which an overlap area between the two sections is optimized to achieve a wide impedance bandwidth. Moreover, by etching two symmetrical quarter-elliptical slots on the ground plane and optimizing the ellipticity ratio, (r_1/r_2), further enhancement in impedance bandwidth is achieved. Although the optimal values of design parameters are obtained thought full-wave HFSS simulations, an initial design can be derived based on simple analytic formulas. For an ellipse of a major radius r_x and a minor radius r_y, the perimeter (unit in millimeters) is given by [22]:

$$p = 4r_x E(k) \tag{1}$$

where $E(k)$ is a complete elliptic integral of the second kind and is defined as:

$$E(k) = \int_0^{\frac{\pi}{2}} \left(1 - k^2 \sin^2\theta\right)^{\frac{1}{2}} d\theta \tag{2}$$

k is called the elliptic modulus and is as follows:

$$k = \sqrt{1 - \left(\frac{r_x}{r_y}\right)} \tag{3}$$

The complete elliptic integral in Eq. (2) can be computed numerically using MATLAB. The lower edge of the impedance bandwidth (unit in GHz) of the antenna is as follows [22]:

$$f_L = \frac{c}{p\sqrt{\frac{1+\varepsilon_r}{2}}} \tag{4}$$

where c is the speed of light in free space.

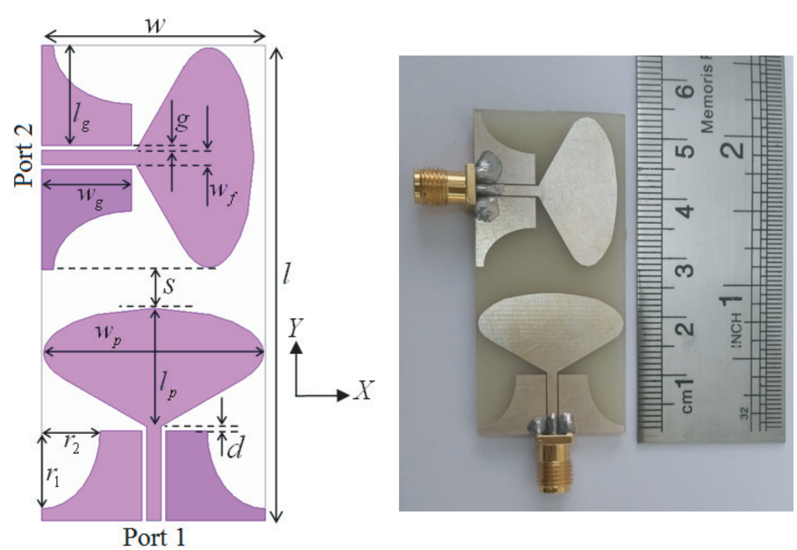

(a) (b)

Figure 1. Geometry and fabricated prototype of the proposed antenna. (a) Antenna geometry and design parameter. (b) Photograph of the fabricated antenna.

3. RESULTS AND DISCUSSION

Figure 2 presents the comparison of experimental and numerical reflection coefficient curves of the antenna. The experimental result shows reasonable concordance with the numerical data. Both measured and simulated results show that the proposed antenna can cover the frequency range of 2.4–18 GHz (153% impedance bandwidth for $|S_{11}| < -10$ dB and $|S_{22}| < -10$ dB) for both ports. The measured and simulated coupling coefficient ($|S_{21}|$) curves of the antenna are shown in Figure 3. As illustrated in this figure, good port isolation above 25 dB over the entire working band is achieved. The slight discrepancy between the experimental and numerical results may be due to the measurement errors. Figure 4 plots the numerical and experimental far-field radiation patterns of the antenna at 3, 10, and 18 GHz when port 2 is matched with a 50 Ω broadband load, while port 1 is excited, and

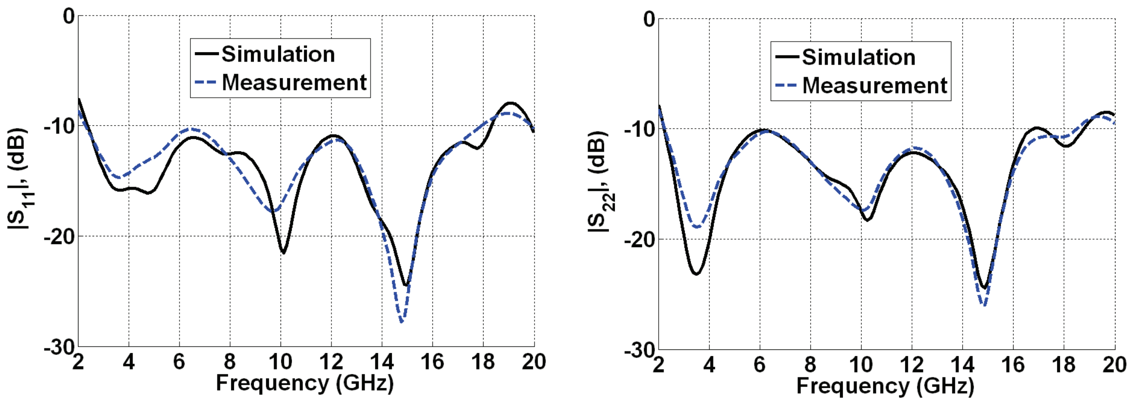

(a) (b)

Figure 2. Experimental and numerical reflection coefficient curves of the antenna. (a) Port 1. (b) Port 2.

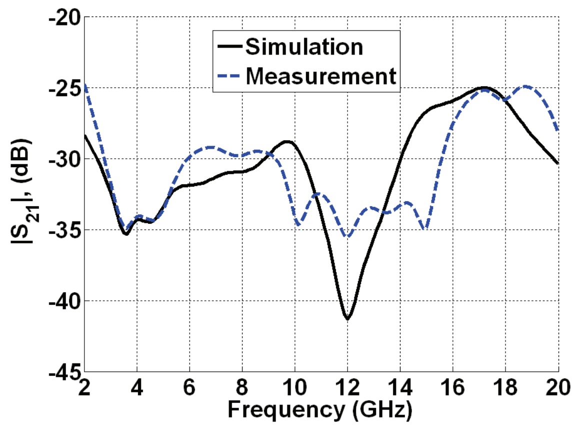

Figure 3. Experimental and numerical isolation (coupling coefficient) curves of the antenna.

vice versa. As shown in this figure, the radiation patterns at port 1 and port 2 are nearly similar with approximately a 90° rotation, showing a good orthogonal polarization operation. Also, the antenna provides almost omnidirectional radiation patterns. Figure 5 depicts the experimental and numerical peak gain curves of the proposed antenna for both ports versus frequency. The average values of the measured gain for ports 1 and 2 are 2.77 and 3.29 dBi, respectively. It should be noted that the gain is reasonable over the working band regardless the small size of the antenna. The discrepancy between the experimental and numerical results may be due to the fabrication tolerances and measurement errors. The experimental and numerical radiation efficiency curves of the antenna for ports 1 and 2 are plotted in Figure 6. It is seen that the fabricated wideband MIMO antenna can provide desirable radiation efficiency of greater than 83% (for both ports) over the entire frequency range of interest. Also, maximum radiation efficiency of the antenna is about 95% which is occurred at the lower edge of the frequency band.

In order to analyze the time-domain performance of the designed broadband MIMO antenna, group delay is investigated. This time-domain characteristic determines the signal distortion which an antenna adds to its input signal. Notice that the signal distortion reduces signal-to-noise ratio and increases bit error rate in communication systems. In a wideband communication system, the group delay is one of the important characteristics. In order to provide desirable time-domain behaviour, constant group delay is required over the entire working band. Figure 7 plots the measured and simulated group delay curves of the antenna for side-by-side case. To investigate the group delay, the distance between the receiving and transmitting antennas was selected as 400 mm. As shown in Figure 7, the peak-to-peak

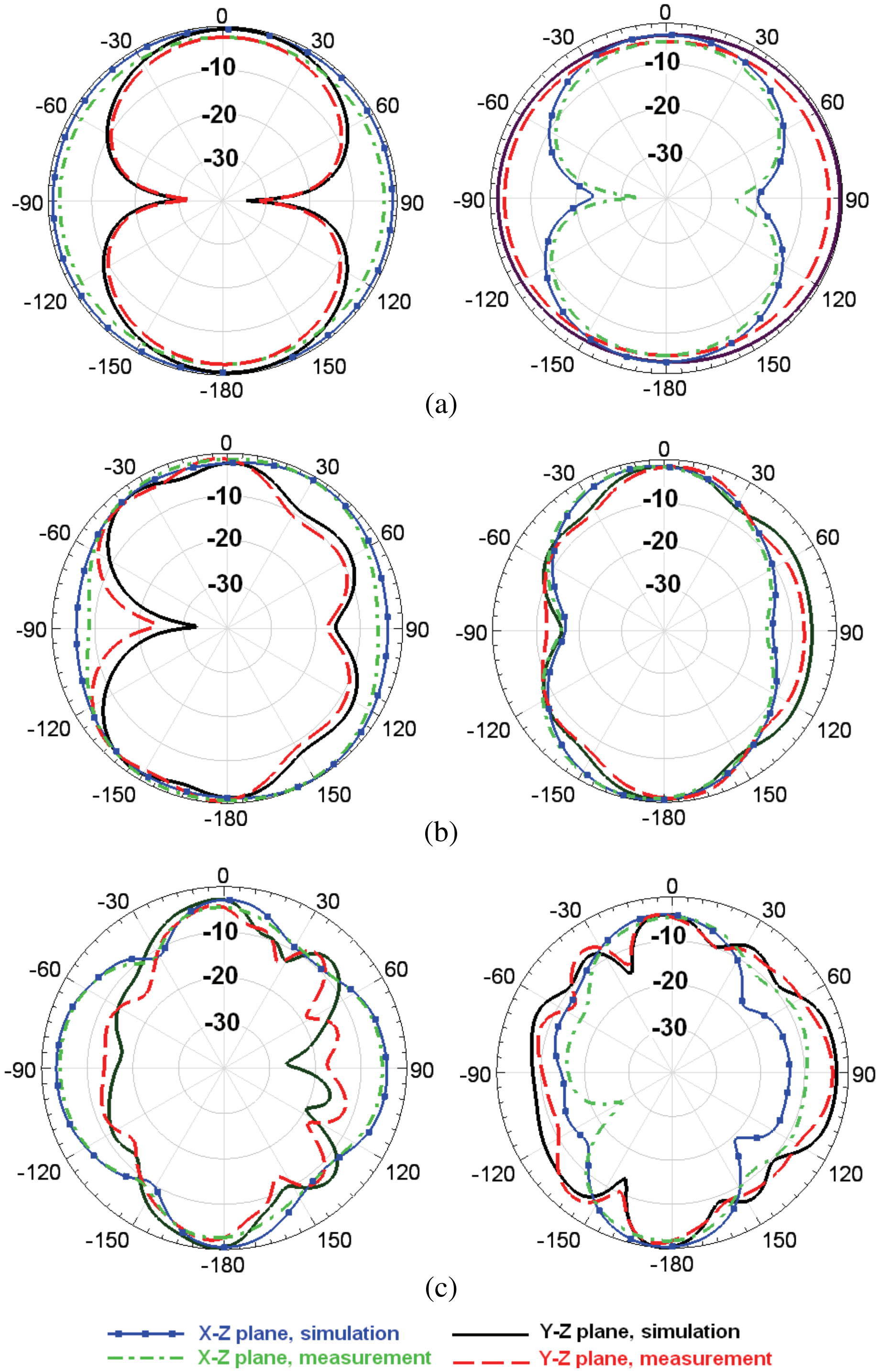

Figure 4. Experimental and numerical radiation patterns of the antenna, left: port 1, right: port 2. (a) 3 GHz. (b) 10 GHz. (c) 18 GHz.

variation of the measured group delay for both ports is less than 1ns over the whole working band. The results indicate that the proposed antenna has an acceptable time domain response without significant distortion. Although not shown, similar results for face-to-face configuration were obtained.

To conclude, the efficiency of the antenna in terms of size, bandwidth, port isolation, radiation efficiency, and group delay is compared with recent wideband dual-polarized antennas presented in [16–

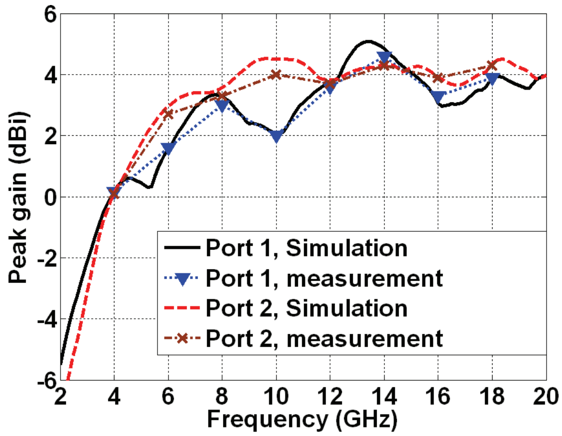

Figure 5. Experimental and numerical gain of the antenna.

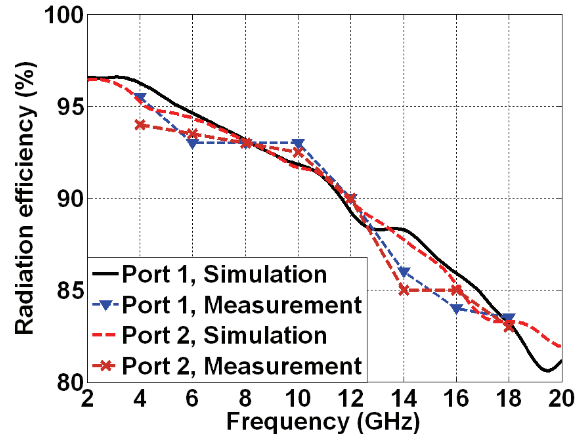

Figure 6. Experimental and numerical radiation efficiency curves of the antenna.

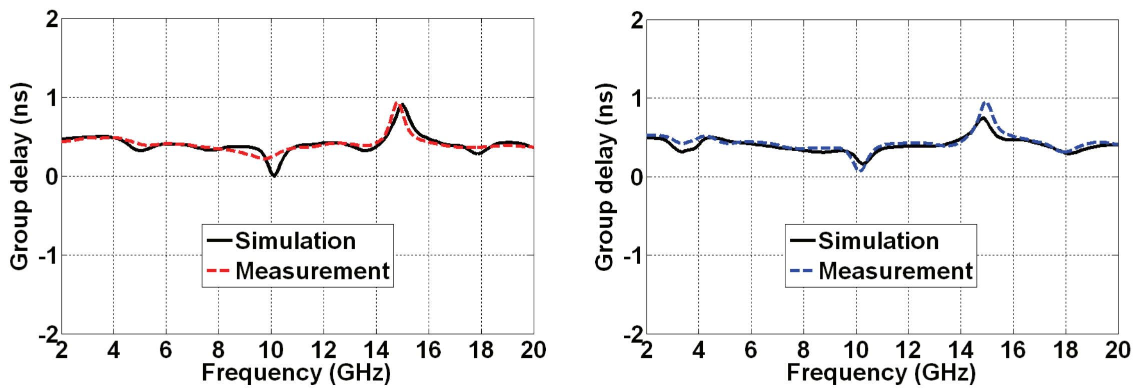

(a) (b)

Figure 7. Experimental and numerical group delay curves of the antenna. (a) Port 1. (b) Port 2.

Table 1. Comparison of the proposed antenna with recent dual-port MIMO antennas.

Reference	Proposed antenna	[16]	[17]	[18]	[19]	[20]
Antenna size (mm^2)	25×53	56×56	80×80	34×49	50×50	27×52
Frequency range (GHz)	2.4–18	3–10.8	3–12	3.1–10.6	2.7–10.8	3.2–12
Impedance bandwidth (%)	153	113	120	109.5	120	115
Port isolation (dB)	> 25	> 20	> 18	> 20	> 15	> 22
Radiation efficiency (%)	> 83	> 62	> 50	------	> 68	------
Group delay variations (ns)	< 1	------	------	< 1	< 1	------

20]. The comparison results are tabulated in Table 1. As shown in this table, compared with the previous design, the proposed antenna has wider overall bandwidth, better port isolation, better time domain response, and smaller size, simultaneously. This comparison reveals the advantages of the antenna.

4. CONCLUSION

A low-profile and wideband planar single-layer dual-port antenna has been proposed for MIMO applications. The antenna includes two identical hybrid trapezoidal-elliptical radiating patches that are printed perpendicular to each other. Also, two orthogonal CPW lines are used to feed the radiating elements. To achieve broadband dual-polarized operation with a compact size, the design parameters of the antenna were optimized by using Ansoft HFSS. The fabricated prototype with a small area of $25 \times 53\,\mathrm{mm}^2$ has the wide operating band from 2.4 to 18 GHz for both ports. The measured isolation between the ports is above 25 dB over the entire band of interest. Besides, the proposed antenna can provide omnidirectional radiation patterns with a worthy orthogonal polarization operation, reasonable gain, high radiation efficiency, and distortionless time domain response. Compared to the recent printed dual-polarized antennas presented in the literatures, the proposed antenna has wider overall bandwidth, better port isolation, better time domain response, and smaller size, simultaneously. Based on the measured time- and frequency-domain results, the proposed antenna is an attractive option for wideband portable MIMO communication devices.

REFERENCES

1. Chacko, B. P., G. Augustin, and T. A. Denidni, "Uniplanar slot antenna for ultrawideband polarization-diversity applications," *IEEE Antennas Wireless Propag. Lett.*, Vol. 12, 88–91, 2013.
2. Zhang, S., K. Zhao, B. Zhu, Z. Ying, and S. He, "MIMO reference antennas with controllable correlations and total efficiencies," *Progress In Electromagnetics Research*, Vol. 145, 115–121, 2014.
3. Sonkki, M., E. Antonino-Daviu, M. Ferrando-Bataller, and E. T. Salonen, "Planar wideband polarization diversity antenna for mobile terminals," *IEEE Antennas Wireless Propag. Lett.*, Vol. 10, 939–942, 2011.
4. Min, K.-S., M.-S. Kim, C.-K. Park, and M. D. Vu, "Design for PCS antenna based on WIBRO-MIMO," *Progress In Electromagnetics Research Letters*, Vol. 1, 77–83, 2008.
5. Yu, X. H., L. Wang, H.-G. Wang, X. Wu, and Y.-H. Shang, "A novel multiport matching method for maximum capacity of an indoor MIMO system," *Progress In Electromagnetics Research*, Vol. 130, 67–84, 2012.
6. Sharawi, M. S., A. B. Numan, and D. N. Aloi, "Isolation improvement in a dual-band dual-element MIMO antenna system using capacitively loaded loops," *Progress In Electromagnetics Research*, Vol. 134, 247–266, 2013.
7. Kyritsi, P., D. C. Cox, R. A. Valenzuela, and P. W. Wolniansky, "Effect of antenna polarization on the capacity of a multiple element system in an indoor environment," *IEEE J. Sel. Areas Commun.*, Vol. 20, 1227–1239, 2002.
8. Svantesson, T., M. A. Jensen, and J. W. Wallace, "Analysis of electromagnetic field polarizations on multiantenna systems," *IEEE Trans. Wireless Commun.*, Vol. 3, 641–646, 2004.
9. Dong, L., H. Choo, R. W. Heath, Jr., and H. Ling, "Simulation of MIMO channel capacity with antenna polarization diversity," *IEEE Trans. Wireless Commun.*, Vol. 4, 1869–1873, 2005.
10. Li, W., W. Lin, and G. Yang, "A compact MIMO antenna system design with low correlation from 1710 MHz to 2690 MHz" *Progress In Electromagnetics Research*, Vol. 144, 59–65, 2014.
11. Mallahzadeh, A. R., S. Es'haghi, and A. Alipour, " Design of an E-shaped MIMO antenna using IWO algorithm for wireless application at 5.8 GHz," *Progress In Electromagnetics Research*, Vol. 90, 187–203, 2009.
12. Krairiksh, M., P. Keowsawat, C. Phongcharoenpanich, and S. Kosulvit, "Two-probe excited circular ring antenna for MIMO application," *Progress In Electromagnetics Research*, Vol. 97, 417–431, 2009.

13. Chou, H.-T., H.-C. Cheng, H.-T. Hsu, and L.-R. Kuo, "Investigation of isolation improvement techniques for multiple input multiple output (MIMO) WLAN portable terminal applications," *Progress In Electromagnetics Research*, Vol. 85, 349–366, 2008.
14. Li, Y., W. X. Li, Ch. Liu, and T. Jiang, "A printed diversity Cantor set fractal antenna for ultra wideband communication applications," *10th International Symposium on Antennas, Propagation and EM Theory (ISAPE)*, 34–38, Xian, China, October 2012.
15. Abbasi, Q. H., M. M. Khan, S. Liaqat, M. Kamran, A. Alomainy, and Y. Hao, "Experimental investigation of ultra wideband diversity techniques for on-body radio communications," *Progress In Electromagnetics Research C*, Vol. 34, 165–181, 2013.
16. Xiong, L. and P. Gao, "Compact dual-polarized slot UWB antenna with CPW-fed structure," *Antennas and Propagation Society International Symposium (APSURSI)*, 1–2, Chicago, IL, USA, July 2012.
17. Gallo, M., E. Antonino-Daviu, M. Ferrando-Bataller, M. Bozzetti, J. M. Molina-Garcia-Pardo, and L. Juan-Llacer, "A broadband pattern diversity annular slot antenna," *IEEE Trans. Antennas Propag.*, Vol 60, No. 3, 1596–1600, 2012.
18. Yoon, H. K., Y. J. Yoon, H. Kim, and C. H. Lee, "Flexible ultra-wideband polarization diversity antenna with band-notch function," *IET Microw. Antennas Propag.*, Vol. 5, No. 12, 1463–1470, 2011.
19. Chacko, B. P., G. Augustin, and T. A. Denidni, "Uniplanar polarization diversity antenna for ultrawideband systems, " *IET Microw. Antennas Propag.*, Vol. 7, No. 10, 851–857, 2013.
20. Koohestani, M., A. A. Moreira, and A. K. Skrivervik, "A novel compact CPW-fed polarization diversity ultrawideband antenna," *IEEE Antennas Wireless Propag. Lett.*, Vol. 13, 563–566, 2014.
21. Dastranj, A., "Low-profile ultra-wideband polarisation diversity antenna with high isolation," *IET Microw. Antennas Propag.*, Vol. 11, No. 10, 1363–1368, 2017.
22. Dastranj, A., "Very small planar broadband monopole antenna with hybrid trapezoidal-elliptical radiator," *IET Microw. Antennas Propag.*, Vol. 11, No. 4, 542–547, 2017.